C5aR2 Deficiency Ameliorates Inflammation in Murine Epidermolysis Bullosa Acquisita by Regulating Fcγ Receptor Expression on Neutrophils

JID Open

Daniel Leonard Seiler[1,2], Marie Kleingarn[1], Katja Hendrika Kähler[1], Caroline Gruner[1], Jovan Schanzenbacher[1], Elvira Ehlers-Jeske[1], Samyr Kenno[1], Christian David Sadik[3,4], Enno Schmidt[3,4,5], Katja Bieber[3,4,5], Jörg Köhl[1,6], Ralf J. Ludwig[3,4,5] and Christian Marcel Karsten[1]

Epidermolysis bullosa acquisita (EBA) is a rare blistering skin disease induced by autoantibodies directed against type VII collagen. The transfer of antibodies against murine type VII collagen into mice mimics the effector phase of EBA and results in a subepidermal blistering phenotype. Activation of the complement system, and especially the C5a/C5aR1 axis driving neutrophil activation, is critical for EBA pathogenesis. However, the role of the alternative C5a receptor, C5aR2, which is commonly thought to be more immunosuppressive, in the pathogenesis of EBA is still elusive. Therefore, we sought to delineate the functional relevance of C5aR2 during the effector phase of EBA. Interestingly, *C5ar2*$^{-/-}$ mice showed an attenuated disease phenotype, suggesting a pathogenic contribution of C5aR2 in disease progression. In vitro, *C5ar2*$^{-/-}$ neutrophils exhibited significantly reduced intracellular calcium flux, ROS release, and migratory capacity when activated with immune complexes or exposed to C5a. These functions were completely absent when *C5ar1*$^{-/-}$ neutrophils were activated. Moreover, C5aR2 deficiency lowered the ratio of activating and inhibitory FcγRs, impeding the sustainment of inflammation. Collectively, we show here a proinflammatory contribution of C5aR2 in the pathogenesis of antibody-induced tissue damage in experimental EBA.

Journal of Investigative Dermatology (2022) **142,** 2715–2723; doi:10.1016/j.jid.2021.12.029

INTRODUCTION

Epidermolysis bullosa acquisita (EBA) is an autoimmune blistering disease of the skin, characterized and caused by autoantibodies targeting type VII collagen (COL7) (Koga et al., 2019; Schmidt and Zillikens, 2013). The activation of the complement system during the effector phase of the disease is considered a central pathogenic process (Kasperkiewicz et al., 2016; Mihai et al., 2018; Sitaru et al., 2005). Activation of complement induces leukocyte extravasation by engagement of leukocyte-expressed complement activation receptors (Ricklin et al., 2010; Tonnesen et al., 1984), and the subsequent release of ROS and proteases within tissues. These events induce tissue damage and eventually degrade the dermal–epidermal adhesion complex (Sadik et al., 2020, 2018). The critical role of the complement system in the pathogenesis of EBA has been confirmed by experiments with mice deficient in the central complement C5. C5 deficiency resulted in a resistance to blister formation in an antibody transfer model of EBA (Sitaru et al., 2005). Furthermore, pharmacological inhibition of C5 recapitulates these findings derived from knockout mice (Sezin et al., 2019). Interestingly, in an experimental model of EBA, only the absence of the G protein-coupled C5aR1, but not of the complement component C6, provided protection from disease development. This suggests that the EBA phenotype observed in *C5*$^{-/-}$ mice can be mainly attributed to the anaphylatoxin C5a and its downstream effector functions, whereas the C5b-dependent formation of the membrane attack complex (C5b-9) is dispensable for the pathogenesis (Karsten et al., 2012; Mihai et al., 2018).

Although C5aR1 is widely recognized as the main signaling receptor for C5a; a second, alternative, receptor exists: C5aR2 (formerly known as C5L2 or GPR77) (Ohno et al., 2000). Initial work on the function of C5aR2 suggested that it might be a decoy receptor with mostly anti-inflammatory effects owing to binding competition with the proinflammatory C5aR1 for C5a. However, there is now widespread agreement that C5aR2 can actively convey

[1]*Institute for Systemic Inflammation Research (ISEF), University of Lübeck, Lübeck, Germany;* [2]*Complement and Inflammation Research Section (CIRS), National Heart, Lung, and Blood Institute (NHLBI), National Institutes of Health (NIH), Bethesda, Maryland, USA;* [3]*Center for Research on Inflammation of the Skin (CRIS), University of Lübeck, Lübeck, Germany;* [4]*Department of Dermatology, Allergy and Venereology, University of Lübeck, Lübeck, Germany;* [5]*Lübeck Institute of Experimental Dermatology (LIED), University of Lübeck, Lübeck, Germany; and* [6]*Division of Immunobiology, Cincinnati Children's Hospital Medical Center, Cincinnati, Ohio, USA*

Correspondence: Christian Marcel Karsten, Institute for Systemic Inflammation Research (ISEF), University of Lübeck, Marie-Curie-Strasse, D-23562 Lübeck, Germany. E-mail: christian.karsten@uksh.de

Abbreviations: A/I ratio, ratio between activating and inhibitory FcγRs; AUC, area under the curve; BM, bone marrow; $(Ca^{2+})_i$, intracellular calcium; COL7, type VII collagen; EBA, epidermolysis bullosa acquisita; IC, immune complex; mCOL7, murine type VII collagen; MFI, mean fluorescence intensity; WT, wild-type

Received 23 February 2021; revised 6 December 2021; accepted 17 December 2021; accepted manuscript published online 7 January 2022; corrected proof published online 21 August 2022

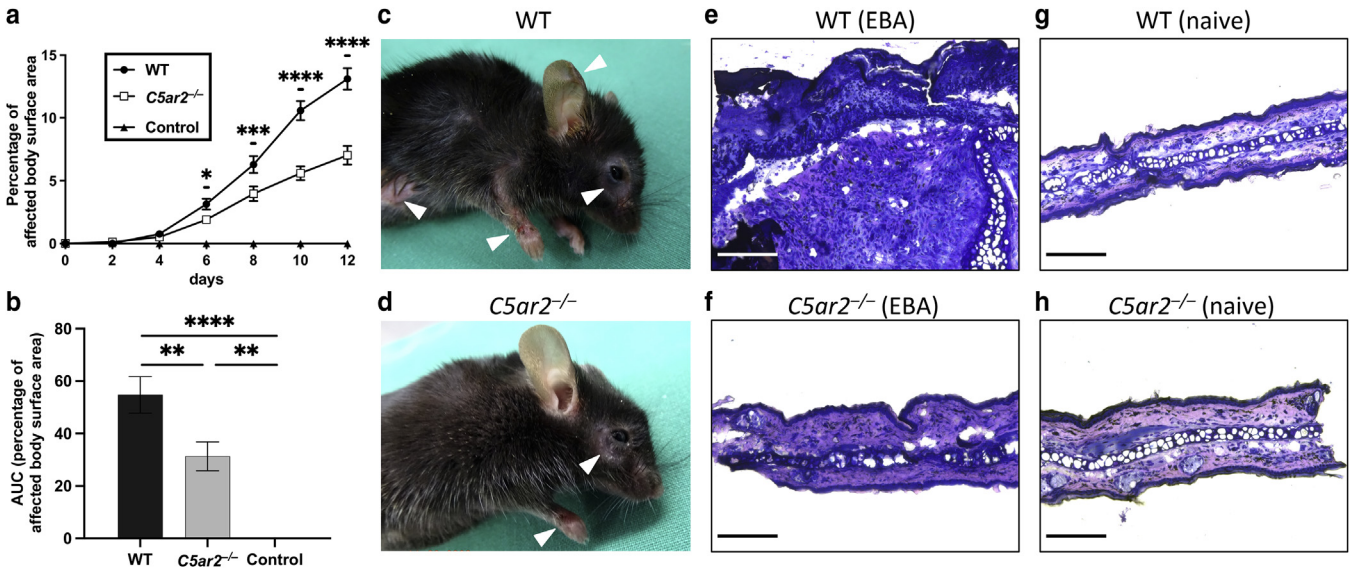

Figure 1. C5aR2 mediates blister formation by anti-mCOL7 IgG. Disease activity was quantified as a percentage of body surface area affected. (**a, b**) Injection of anti-mCOL7 IgG in *C5ar2*$^{-/-}$ mice resulted in significantly fewer EBA skin lesions than in WT mice (n = 15 per group). Injection of Dulbecco's PBS in WT control mice (n = 8) did not result in spontaneous disease development. Representative pictures of clinical lesions are shown in (**c**) WT mice and (**d**) *C5ar2*$^{-/-}$ mice. Histopathology revealed evident inflammation in the skin of (**e**) WT mice but minimal in the skin of (**f**) *C5ar2*$^{-/-}$ mice compared with the representative skin sections of naive, nondiseased (**g**) WT, and (**h**) *C5ar2*$^{-/-}$ mice. Bar = 100 mm. Differences in disease activity were analyzed by two-way ANOVA for (**a**) or ordinary one-way ANOVA for (**b**), with Holm-Šídák multiple comparisons test. AUC, area under the curve; EBA, epidermolysis bullosa acquisita; mCOL7, murine type VII collagen; WT, wild-type. *$P < 0.05$, **$P < 0.01$, ***$P < 0.001$, ****$P < 0.0001$.

immunomodulatory signals and modulate cellular responses (Bamberg et al., 2010; Croker et al., 2014; Kalant et al., 2005; Van Lith et al., 2009). Unlike C5aR1, C5aR2 does not engage intracellularly with G proteins and therefore signals in a G protein-independent fashion (Okinaga et al., 2003). However, C5aR2 can directly recruit β-arrestin 2 and also modulate the recruitment of β-arrestin 2 to C5aR1 (Croker et al., 2014; Kalant et al., 2005). The C5aR2−β-arrestin 2 interaction results in decreased C5a-mediated extracellular signal−regulated kinase 1/2 phosphorylation and lipopolysaccharide-induced production of IL-6 in myeloid cells (Croker et al., 2016). Furthermore, C5aR2 has been shown to oppositely modulate disease progression in a pro- (Poppelaars et al., 2017; Rittirsch et al., 2008; Thorenz et al., 2018; Zhang et al., 2010) or anti-inflammatory (Gerard et al., 2005; Wang et al., 2013; Wu et al., 2020) manner in various inflammatory models, depending on the disease model studied (Zhang et al., 2017).

Neutrophils drive cellular effector responses in a range of antibody-mediated diseases, including EBA (Chiriac et al., 2007; Girardi et al., 2003; Looney et al., 2006; Samavedam et al., 2014; Sezin et al., 2017; Shimanovich et al., 2004; Sitaru et al., 2005; Wipke and Allen, 2001). Because we previously noted a high expression of C5aR2 on neutrophils (Karsten et al., 2017), we investigated the previously unexplored potential role of C5aR2 in experimental EBA.

RESULTS

Experimental EBA is ameliorated in *C5ar2*$^{-/-}$ mice

C5ar2$^{-/-}$ and wild-type (WT) mice were injected with affinity-purified rabbit IgG directed against murine COL7 (mCOL7) to induce experimental EBA. Mice of both genotypes showed first clinical signs of skin blistering from day 4 onward after anti-mCOL7 IgG injection. However, disease progression was ameliorated in *C5ar2*$^{-/-}$ mice from day 6 onward (Figure 1a), and by day 12, *C5ar2*$^{-/-}$ mice displayed significantly reduced areas of blister-affected skin (7.6 ± 0.7%) compared with that in WT mice (13.1 ± 0.8%). Accordingly, the cumulative disease severity, expressed as area under the curve (AUC) over time, was also significantly reduced in *C5ar2*$^{-/-}$ mice (Figure 1b). Skin blisters and signs of inflammation were also evident in lesional skin sections of the ear, characterized by tissue swelling and cellular infiltration (Figure 1e−h), suggesting strongly disseminated disease (Figure 1c and d).

Anti-mCOL7 IgG and C3b deposition at the dermal−epidermal junction are not altered in *C5ar2*$^{-/-}$ mice

To exclude the possibility that the observed difference in disease activity between WT and *C5ar2*$^{-/-}$ mice may be due to inherent changes of IgG deposition or complement activation in the knock-out animals, cryosections from ears were examined by direct immunofluorescence microscopy for COL7 IgG and C3b deposition at the dermal−epidermal junction. We observed no significant differences between C5aR2-sufficient or -deficient mice for rabbit anti-mCOL7 IgG or C3b deposits at the dermal−epidermal junction (Figure 2).

Neutrophils from *C5ar2*$^{-/-}$ mice show significantly reduced cellular activation on stimulation with C5a

Neutrophils abundantly express C5aR2 and are central to EBA development. We therefore next assessed whether neutrophils lacking C5aR2 may respond differently to stimulation with C5a. For this, bone marrow (BM) cells were isolated from naive, nondiseased WT or *C5ar2*$^{-/-}$ mice and

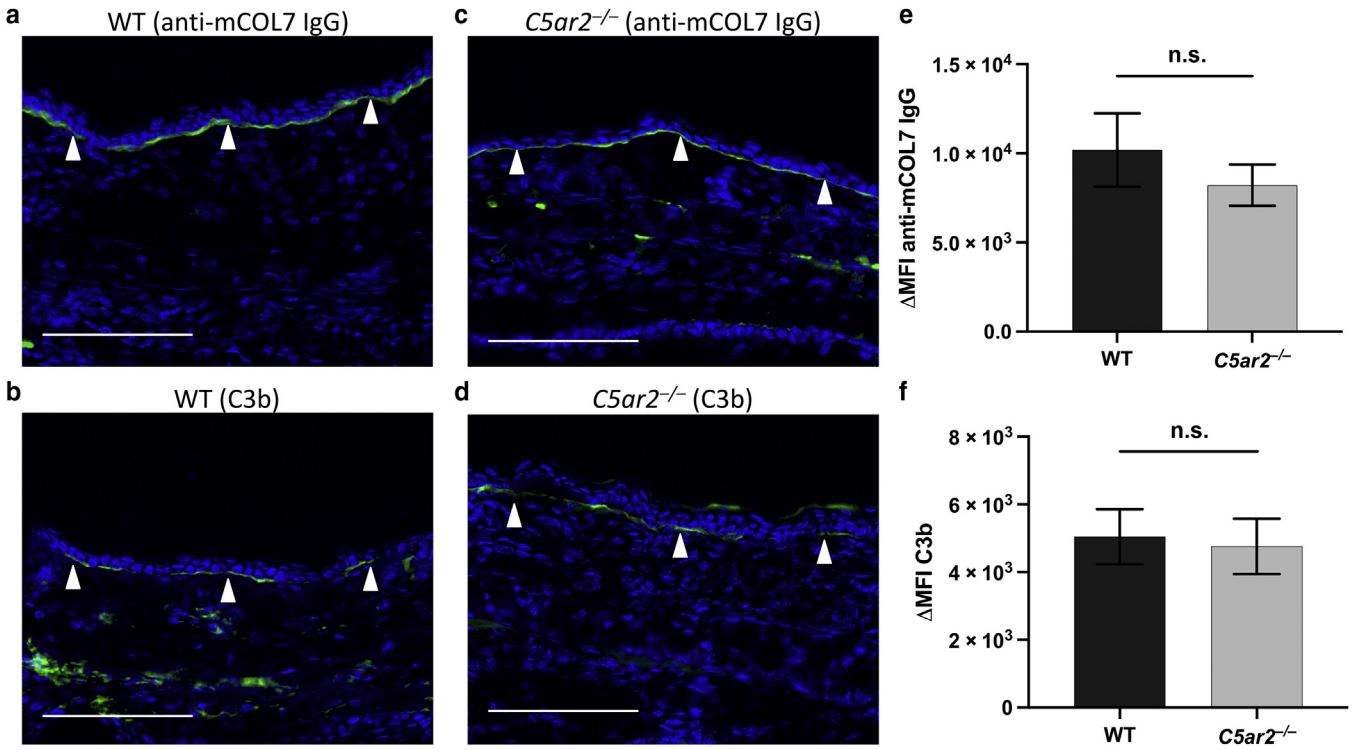

Figure 2. DIF staining for IgG and C3b deposition at the DEJ. DIF staining shows no significant differences in the deposition of anti-mCOL7 IgG and C3b deposits at the DEJ as quantified with ImageJ software. Linear deposits of anti-mCOL7 IgG in biopsies of (**a**) WT and (**c**) *C5ar2*$^{-/-}$ mice, as revealed by DIF. Activation of the complement system indicated by deposition of C3b along the DEJ in biopsies from (**b**) WT and (**d**) *C5ar2*$^{-/-}$ mice. Bar = 100 μm. For demonstration purposes, brightness and contrast were adjusted in the entire image to highlight IgG and C3b deposition. Quantitative evaluation of (**e**) anti-mCOL7 IgG (n = 15) and (**f**) C3b deposition (n = 12), indicated by the background-corrected ΔMFI values in biopsies of ear skin, was performed in images without post-processing. Differences between groups were analyzed by unpaired two-tailed *t*-test. DEJ, dermal–epidermal junction; DIF, direct immunofluorescence; mCOL7, murine type VII collagen; MFI, mean fluorescence intensity; n.s., not significant; WT, wild-type.

examined for C5a-mediated effector functions as indicated by an increase in intracellular calcium $(Ca^{2+})_i$ flux and upregulation of CD11b; events normally induced by neutrophils exposed to C5a. Ly6G$^+$ BM cells (Figure 3a) lacking C5aR2 showed a significantly blunted $(Ca^{2+})_i$ flux compared with Ly6G$^+$ BM cells isolated from WT mice (WT: 44.3 ± 5.0%; *C5ar2*$^{-/-}$: 20.3 ± 4.1%). As expected, neutrophils derived from *C5ar1*$^{-/-}$ mice displayed fully abrogated $(Ca^{2+})_i$ flux after C5a stimulation (Figure 3b). We made similar observations when measuring surface expression levels of CD11b after stimulation with C5a: Ly6G$^+$ BM cells from *C5ar2*$^{-/-}$ mice showed a strong reduction in CD11b upregulation (171.2 ± 19.5%) compared with Ly6G$^+$ BM cells from WT mice (214.3 ± 9.3%), whereas CD11b surface expression in Ly6G$^+$ BM cells from *C5ar1*$^{-/-}$ mice remained nondetectable after stimulation with C5a (Figure 3c). These findings were also confirmed for Ly6G$^+$ cells from the BM of WT and *C5ar2*$^{-/-}$ mice after EBA induction (Supplementary Figure S1a and b).

Thus, these data show that neutrophils, devoid of C5aR2 expression, have a reduced activation profile on stimulation with C5a in vitro.

Immune complex-induced ROS release is significantly decreased in *C5ar2*$^{-/-}$ neutrophils

To determine whether the difference in the disease activity between WT and *C5ar2*$^{-/-}$ mice may also be due to diminished ROS release by *C5ar2*$^{-/-}$ neutrophils, ROS release by isolated BM cells was analyzed after stimulation with an immune complex (IC) composed of mCOL7C and rabbit anti-mCOL7 IgG, mimicking the disease-inducing IC in the EBA mouse model. BM cells from naive, nondiseased mice of both genotypes released ROS within the first 30 minutes after stimulation with the IC (data not shown). However, relative ROS release by neutrophils from *C5ar2*$^{-/-}$ mice was significantly decreased (relative AUC: 2.09 ± 0.26) compared with cells from WT mice (relative AUC: 2.61 ± 0.23; Figure 3d).

Thus, these data show that the loss of C5aR2 expression on neutrophils results in decreased ROS release on stimulation with ICs in vitro.

Neutrophils lacking C5aR2 show significantly lower migration toward C5a

We next assessed whether the migratory capacity toward a C5a gradient may also be affected by C5aR2 deficiency, using an established in vitro transwell migration experiment. Indeed, the percentage of chemotactic Ly6G$^+$ BM cells was significantly lower in *C5ar2*$^{-/-}$ mice (28.5 ± 4.0%) compared with that in corresponding cells isolated from WT mice (40.3 ± 4.6%). Approximately 9.5 ± 1.6% of seeded Ly6G$^+$ BM cells derived from *C5ar1*$^{-/-}$ control mice transmigrated into the bottom well, which basically represented the baseline or background value (control: 9.9 ± 1.3%; Figure 3e). To probe for neutrophil migration in vivo, the number of neutrophils in the blood and among the infiltrating

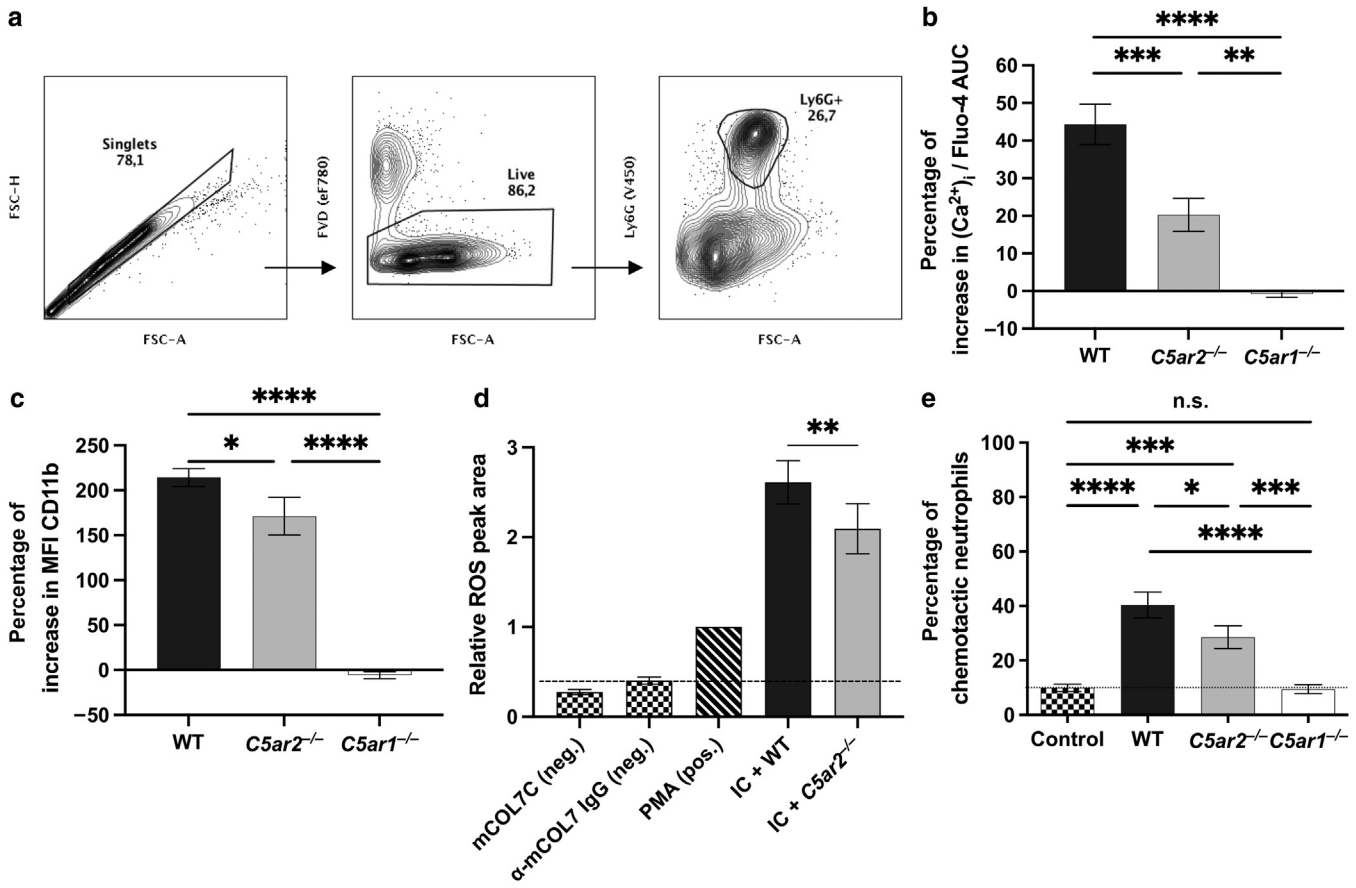

Figure 3. C5a-mediated activation potential and migration behavior is significantly diminished in neutrophils of *C5ar2*$^{-/-}$ mice. (**a**) Flow cytometric gating strategy to identify neutrophils as Ly6G$^+$ live BM cells from naive, nondiseased mice. (**b**) C5a-dependent changes in $(Ca^{2+})_i$ concentration as an indicator of cellular activation quantified by changes in fluorescence intensity of the calcium-sensitive compound Fluo-4 over the time (n = 8 per group). (**c**) C5a-mediated activation of neutrophils quantified by upregulation of surface expression of CD11b (n ≥ 8 per group). (**d**) IC-induced release of ROS from BM cells (n ≥ 9 per group). (**e**) Percentage of chemotactic Ly6G$^+$ BM cells in an in vitro migration assay toward C5a (n = 5 per group). Shown are combined data from at least three independent experiments, each performed with 2−3 mice per genotype. Differences between groups were analyzed by ordinary one-way ANOVA with Holm-Šídák multiple comparisons test for (**b**–**e**). AUC, area under the curve; BM, bone marrow; $(Ca^{2+})_i$, intracellular calcium; FSC, forward scatter; FVD, fixable viability dye; IC, immune complex; mCOL7, murine type VII collagen; mCOL7C, recombinant murine type VII collagen C; MFI, mean fluorescence intensity; neg., negative control; n.s., not significant; pos., positive control; WT, wild-type. *$P < 0.05$, **$P < 0.01$, ***$P < 0.001$, ****$P < 0.0001$.

cells into the ears of WT and *C5ar2*$^{-/-}$ mice was quantified after EBA induction. Blood neutrophil count and infiltrating immune cells in the ears of diseased mice were significantly higher than that in naive, nondiseased WT control mice (Supplementary Figure S2). We also noted a nonsignificant trend toward higher immune cell numbers in WT mice than the numbers in *C5ar2*$^{-/-}$ mice, 12 days after EBA induction (Supplementary Figure S2).

C5aR1 expression in neutrophils is not altered by C5aR2 deficiency

To determine whether the effects on the activation potential and the migration behavior observed in the different in vitro-settings were due to an effect of C5aR2 deficiency on C5aR1 (CD88) expression, surface expression of C5aR1 on neutrophils of the different genotypes was assessed by flow cytometry. As shown in Figure 4a, C5aR1 expression in Ly6G$^+$ neutrophils from naive, nondiseased *C5ar2*$^{-/-}$ mice was similar to that in WT mice. These findings were also confirmed for Ly6G$^+$ cells from BM of diseased mice (Supplementary Figure S1c).

Neutrophils from *C5ar2*$^{-/-}$ mice exhibit an altered ratio of activating and inhibitory FcγRs

Previous studies showed that subepidermal blister formation depends on the interaction between COL7/anti-mCOL7 IgG ICs and activating FcγRs, namely FcγRIII and FcγRIV, whereas inhibitory FcγRIIb is protective in EBA (Kasperkiewicz et al., 2012; Kovacs et al., 2020). Therefore, we analyzed the expression profiles of FcγRIIb, FcγRIII, and FcγRIV on neutrophils from WT and *C5ar2*$^{-/-}$ mice in the nondiseased state. The respective expression profiles of the activating receptors, FcγRIII and FcγRIV, were comparable between WT and *C5ar2*$^{-/-}$ mice in the steady state. However, surface expression of FcγRIIb was significantly augmented in Ly6G$^+$ BM cells isolated from naive, nondiseased *C5ar2*$^{-/-}$ mice when compared with that in the corresponding cells from WT mice. This effect was not observed in neutrophils from *C5ar1*$^{-/-}$ mice, which maintained unchanged expression of FcγRs compared with those from WT mice (data not shown). Specifically, surface expression of FcγRIIb was more than 3-fold increased on Ly6G$^+$ BM cells from naive, nondiseased *C5ar2*$^{-/-}$ mice (mean fluorescence intensity [MFI]:

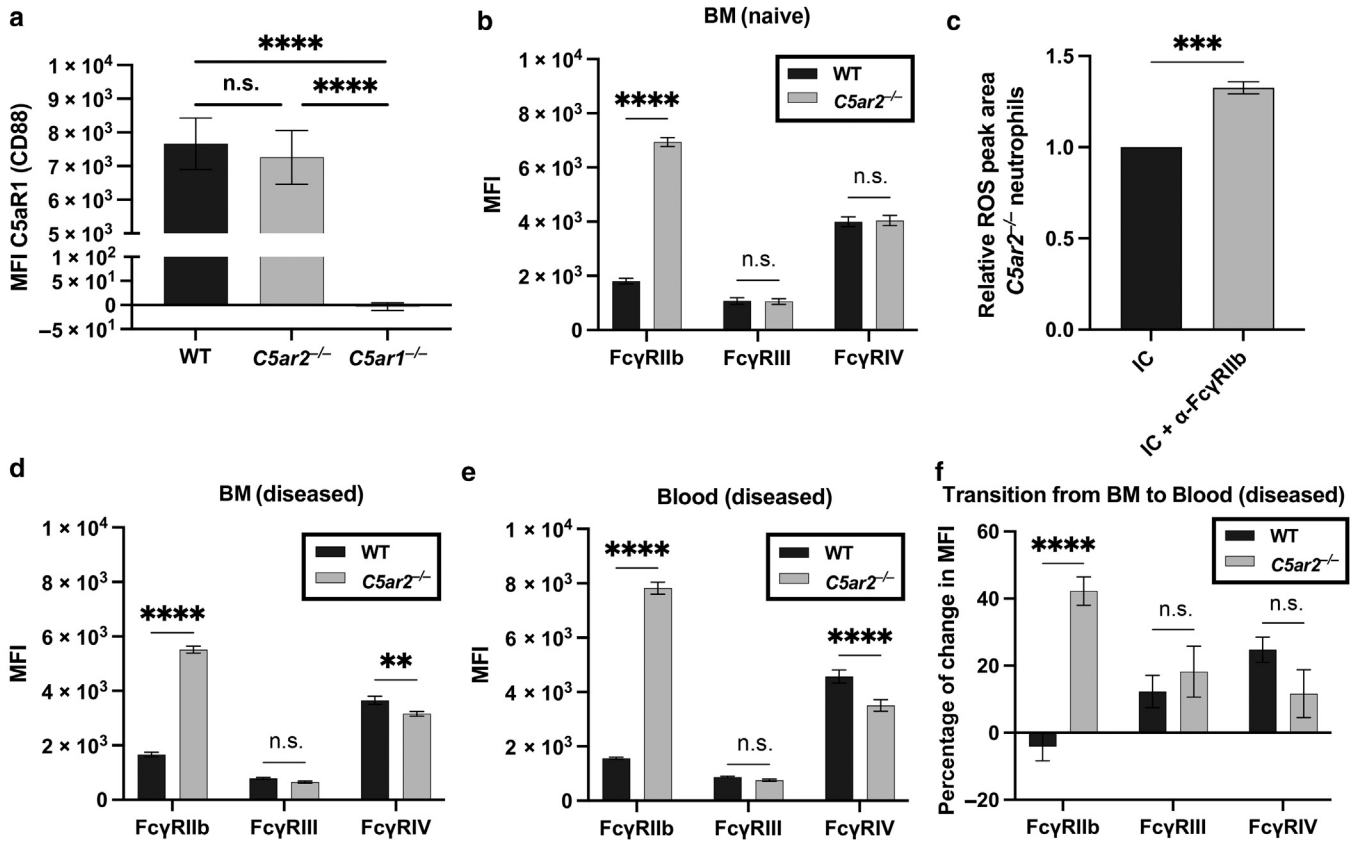

Figure 4. C5aR2 deficiency has no effect on C5aR1 expression but lowers the A/I ratio of FcγRs. Quantitative assessment of (**a**) C5aR1 and (**b**) FcγRs surface expression ($n \geq 8$ per group) in Ly6G$^+$ BM cells from naive, nondiseased mice. (**c**) Effect of antibody-mediated blockade of FcγRIIb on ROS release by BM cells from naive, nondiseased *C5ar2*$^{-/-}$ mice ($n = 3$ per group). FcγRs expression in Ly6G$^+$ (**d**) BM and (**e**) blood cells from diseased mice. (**f**) Percentage change in FcγRs expression after the transition of Ly6G$^+$ cells from BM to blood in diseased mice. Shown are combined data from at least three (**a, b**) or two (**d**–**f**) independent experiments, each performed with 2–3 (**a, b**) or 5 (**d**–**f**) mice per genotype. Differences between groups were analyzed by unpaired one-tailed *t*-test for (**c**), ordinary one-way ANOVA for (**a**), and two-way ANOVA for (**b, d**–**f**), with Holm-Šídák multiple comparisons test. A/I ratio, ratio between activating and inhibitory FcγRs; BM, bone marrow; IC, immune complex; MFI, mean fluorescence intensity; n.s., not significant; WT, wild-type. $^{**}P < 0.01$, $^{***}P < 0.001$, $^{****}P < 0.0001$.

6,936 ± 159) compared with WT cells (MFI: 1,806 ± 102; Figure 4b). Consequently, the ratio between activating and inhibitory FcγRs (A/I ratio), that is, the balance between activating and inhibitory FcγRs, was tipped toward the inhibitory receptor in neutrophils lacking C5aR2. This altered balance contributed to the muted ROS release by neutrophils from *C5ar2*$^{-/-}$ mice, as the blockade of FcγRIIb by an inhibitory antibody rescued ROS release in IC-stimulated *C5ar2*$^{-/-}$ neutrophils: ROS release from *C5ar2*$^{-/-}$ BM cells was increased by 32.6 ± 2.7% after the blockade of FcγRIIb (Figure 4c).

To verify whether the lower A/I ratio of FcγRs expression by neutrophils from *C5ar2*$^{-/-}$ mice is sustained on EBA disease induction, the expression of FcγRs on neutrophils from BM and blood of diseased mice was analyzed 12 days after anti-mCOL7 IgG injection. Neutrophils from both sites in the *C5ar2*$^{-/-}$ mice showed a significant increase in FcγRIIb expression (MFI BM: 5,515 ± 124; MFI blood: 7,826 ± 212). Furthermore, different from nondiseased mice, FcγRIV expression was significantly lower in both Ly6G$^+$ cells of the BM (MFI: 3,115 ± 78) and blood (MFI: 3,785 ± 256; Figure 4d) from diseased *C5ar2*$^{-/-}$ mice compared with that in the matching cells from WT mice. In addition, Ly6G$^+$ BM cells from diseased mice of both genotypes increased the expression of activating FcγRs, FcγRIII and FcγRIV, after BM to blood transition. However, blood neutrophils from diseased WT mice showed a slightly decreased expression of FcγRIIb compared with their BM counterparts, whereas blood neutrophils from diseased *C5ar2*$^{-/-}$ mice further increased their FcγRIIb expression and reached a 5-fold increase in FcγRIIb expression (MFI: 7,826 ± 212) compared with the corresponding WT mice (MFI: 1,563 ± 36; Figure 4e-f).

Thus, these data show that C5aR2 deficiency shifts the A/I ratio on neutrophils toward an inhibitory phenotype, resulting in decreased IC-induced ROS release.

DISCUSSION

Insight into the pathogenesis of EBA has been gained by the use of animal models (Bieber and Ludwig, 2020; Kasprick et al., 2019; Nishie, 2014). The antibody transfer animal model has been utilized to discover and define the importance of C5aR1 in the pathogenesis of EBA (Karsten et al., 2012; Mihai et al., 2018). The main objective of this study was to elucidate whether C5aR2 has functional properties relevant to the progression of EBA. For this purpose, we also

chose the antibody transfer EBA mouse model, which mimics the effector phase of the disease.

The finding that disease activity was significantly lower in *C5ar2*$^{-/-}$ mice than in WT mice was surprising because C5aR2 had previously been shown to be protective in an antibody transfer model of bullous pemphigoid (Karsten et al., 2018). This difference might be explained by the fact that the pathomechanisms in bullous pemphigoid are slightly different from those in EBA with autoantibodies directed against the hemidesmosomal components BP180 (type XVII collagen) and BP230 (Schmidt and Zillikens, 2013). This notion is supported by the different roles of FcγRIII and C5 in the two antibody transfer mouse models. Although in the EBA model, only FcγRIV, but not FcγRIII, is relevant for antibody-mediated tissue destruction, and *C5*$^{-/-}$ mice are almost completely protected (Kasperkiewicz et al., 2012; Sitaru et al., 2005); in the bullous pemphigoid mouse model, both FcγRIII and FcγRIV drive tissue destruction, and *C5*$^{-/-}$ mice showed a decrease in skin lesions by 50% compared with WT mice (Karsten et al., 2018; Schulze et al., 2014). In addition and in contrast to this study, the aforementioned study used *C5ar2*$^{-/-}$ and WT mice on a *BALB/c* background. Interestingly, WT mice on a *C57BL/6* background developed stronger signs of skin blistering than WT mice on a *BALB/c* background (Karsten et al., 2018), which might be explained by the differences in the C5 circulating levels between these strains (Lajoie et al., 2010).

Lipid and complement mediators have previously been shown to influence the course of pathogenesis of (auto-) antibody-induced diseases by modulating the infiltration of effector cells into the skin (Koga et al., 2019; Sadik et al., 2012; Sezin et al., 2017). Among the complement components involved, C5a, the most potent anaphylatoxin of our immune system, plays a key role. Therefore, reduced mobilization and/or recruitment of neutrophils into the skin was initially a plausible potential explanation for the reduced EBA disease activity in *C5ar2*$^{-/-}$ mice. Moreover, in *C5ar2*$^{-/-}$ mice, reduced inflammation was also noted in models of thioglycolate peritonitis and intestinal ischemia–reperfusion injury, which also depend on normal neutrophil migration (Chen et al., 2007; Wu et al., 2020). In addition, mobilization of neutrophils from the BM is impaired in *C5ar2*$^{-/-}$ mice (Wu et al., 2020). In IC-induced arthritis, C5aR2 is required for the trans-epithelial transport of tissue-derived C5a into the blood lumen to induce leukocyte entry into the joint (Miyabe et al., 2019). Although BM-derived neutrophils from naive, non-diseased *C5ar2*$^{-/-}$ mice showed a significantly reduced chemotaxis toward C5a in vitro (Figure 3e), we unexpectedly only observed a nonstatistical trend toward reduced numbers of neutrophils in the blood and skin of diseased *C5ar2*$^{-/-}$ mice compared with that in the blood and skin of WT mice (Supplementary Figure S2). The reasons for this finding are still unclear; however, it is possible that in this particular in vivo disease model, C5aR1 activity mediates neutrophil migration successfully. Of note, in a previous work, we found no significant reduction in the chemotactic activity of neutrophils from *C5ar2*$^{-/-}$ mice compared with that of neutrophils from WT mice in vitro (Karsten et al., 2018). This discrepancy is best explained by the different detection methods used to enumerate migrated neutrophils, namely the manual counting previously and flow cytometry in this study, which constitutes a more sensitive and unbiased approach.

Nonetheless, we found that C5a-induced cellular activation was significantly reduced in neutrophils from *C5ar2*$^{-/-}$ mice compared with that in neutrophils from WT mice, consistent with previous data showing impaired C5a-mediated Mac-1 (CD11b/CD18) induction in *C5ar2*$^{-/-}$ neutrophils (Chen et al., 2007). Moreover, C5a-induced cellular activation was completely absent in *C5ar1*$^{-/-}$ neutrophils, supporting the notion that C5aR1 engagement by C5a is mandatory for normal neutrophil activity in these experimental settings. Considering the known signaling intersections between C5aR1 and C5aR2 among several cell types, and the strong reduction in *C5ar2*$^{-/-}$ neutrophil (which express C5aR1) activation, it is likely that C5aR2 stimulation enhances C5aR1 activities. This enhancing effect may result from heterodimer formation between the two C5a receptors as previously described but clearly requires future experimental exploration (Croker et al., 2014, 2013).

Excitingly, we found a second mechanism that accounts for blunted neutrophil activity in *C5ar2*$^{-/-}$ mice. Neutrophils from *C5ar2*$^{-/-}$ animals exhibited a strong decrease in the A/I ratio of FcγRs (Figure 4b, d, and e), which is known to suppress inflammation triggered by (auto-) antibodies (Bussel, 2000; Nimmerjahn and Ravetch, 2008). It has been previously proposed that there is critical bidirectional crosstalk between C5a and FcγR activation on cells expressing both receptor families, including neutrophils. According to previously observed data, IC-induced generation of C5a can lead to upregulation of activating FcγRs and downregulation of inhibitory FcγRIIb on myeloid cells (Godau et al., 2004; Karsten et al., 2012; Kumar et al., 2006; Shushakova et al., 2002). The ensuing change in the A/I ratio toward the activating phenotype thus primes cells for an inflammatory response through a self-amplifying feedback loop (Atkinson, 2006; Karsten and Köhl, 2012; Kumar et al., 2006; Schmidt and Gessner, 2005). Furthermore, it has been proposed that the crosstalk between C5a and FcγRs on neutrophils not only triggers cellular activation but also sustains neutrophil recruitment in vivo (Sadik et al., 2012). Using a mouse model of IC-induced arthritis, it has been shown that activation of C5a receptor(s) on neutrophils leads to the release of LTB_4 and early recruitment of neutrophils to the joint, whereas FcγR engagement on neutrophils induces the release of IL-1β and subsequent production of chemokines, to ensure sustained tissue inflammation (Chou et al., 2010; Sadik et al., 2012). Our data suggest that, at least in the EBA model, C5aR2 normally supports this IC/C5a-induced inflammatory priming, mainly through altering the expression of FcγRs.

Clearly, further studies are needed to elucidate the underlying molecular mechanisms of FcγR regulation by C5aR2 in inflammatory diseases. This may be especially relevant as the magnitude of FcγRs immune response modulation is strictly isotype-dependent (Nimmerjahn and Ravetch, 2006).

In summary, our study shows that C5aR2 is critically involved in the pathogenesis of EBA. The disease phenotype of *C5ar2*$^{-/-}$ mice in the antibody transfer EBA model partially resembles to that observed in *C5ar1*$^{-/-}$ mice in the same model but in a more muted form (Mihai et al., 2018). Our data indicate that C5aR1 is the major control node here, but

C5aR2 enhances or supports C5aR1-driven EBA pathologies. In addition, we also found a previously unknown regulatory function of C5aR2, specifically the regulation of FcγR expression levels. Together, these C5aR2 functions sustain the recruitment and activation of neutrophils in EBA. Deciphering the molecular mechanisms driving this regulatory function of C5aR2 may be key to uncovering novel pathways of the bidirectional crosstalk between C5a and FcγRs, which will then provide information for future approaches to develop new therapeutic strategies for the treatment of C5a-dependent neutrophil-driven (autoimmune) diseases like EBA.

MATERIALS AND METHODS

Mice and study approval

C57BL/6J (WT) and *C5ar2*$^{-/-}$ mice on the *C57BL/6J* genetic background were bred and housed in a 12-hour light-dark cycle at the University of Lübeck animal facility (Lübeck, Germany). All injections were performed on 8- to 12-week-old anesthetized mice of both sexes. Animal experiments were conducted in strict compliance with the German regulations of the Society for Laboratory Animal Science and the European Health Law of the Federation of Laboratory Animal Science Associations. All animal experiments were approved by the respective local ethics committees for animal experiments of the state of Schleswig-Holstein (Ministerium für Energiewende, Landwirtschaft, Umwelt, Natur und Digitalisierung des Landes Schleswig-Holstein). The approval number is 106-10/19.

Antibody transfer-induced EBA mouse model

Affinity-purified rabbit anti-mCOL7 IgG or normal rabbit serum IgG (see Supplementary Materials and Methods) was injected subcutaneously in *C57BL/6J* (WT) and *C5ar2*$^{-/-}$ (on *C57BL/6J* background) mice of both sexes every other day for a period of four days (three injections in total) in individual doses of 100 μg IgG. Beginning with the first injection (day 0), mice were weighed and examined every other day for general condition and evidence of cutaneous lesions (i.e., erythema, blisters, erosions, and crusts). Cutaneous lesions were scored as skin surface involvement, as previously described (Kasprick et al., 2019). Blood was drawn on day 12, and both lesional and perilesional biopsies (stored at −80 °C) were collected for histopathologic analysis and direct immunofluorescence. Blood samples were prepared for quantitative immunophenotyping by flow cytometry.

Histopathology

Sections (6 μm) from ear skin samples were collected and differentially stained using the Kwik-Diff Stain Kit (Thermo Fisher Scientific, Waltham, MA) following the manufacturer's protocol. Staining was analyzed using a Keyence BZ-X810 all-in-one fluorescence microscope (Keyence, Osaka, Japan) and BZ-X800 viewer software (Keyence), applying white balance to the whole image.

Immunofluorescence microscopy

Tissue-bound antibodies and complement deposition (C3b) were detected by direct immunofluorescence of frozen sections (8 μm) in TissueTek (Sakura Finetek Germany, Staufen im Breisgau, Germany), using FITC-conjugated swine anti-rabbit IgG (8.33 μg/ml; Dako Deutschland, Hamburg, Germany) and FITC-conjugated murine anti-mouse C3 (66.6 μg/ml; MP Biomedicals, Solon, OH), respectively. The compared samples were stained on the same day to exclude influences of day-to-day variations.

Staining was evaluated using a Keyence BZ-X810 all-in-one fluorescence microscope and BZ-X800 viewer software with identical settings for all samples. MFIs corresponding to the deposition of rabbit IgG and C3b were quantified in the acquired images without post-processing, using the ImageJ software (http://rsbweb.nih.gov/ij/; National Institutes of Health, Bethesda, MD), as previously described (Kovacs et al., 2020). Briefly, the dermal–epidermal junction as the site of deposition of IgG and C3b was identified in a bright field. Staining intensities at the dermal–epidermal junction were measured with the area tool, and a reference area of the epidermis was subtracted from this value to determine background-corrected ΔMFI–anti-mCOL7 IgG or ΔMFI-C3b intensity values.

BM cell preparation

Mouse BM cells were isolated as previously described (Karsten et al., 2014). Briefly, BM cells were isolated from femurs and tibiae by flushing the bones with Dulbecco's PBS using a 27G needle. After passing through a 40-μm cell strainer, red blood cells were lysed with hypotonic red blood cell lysis buffer (155 mM ammonium chloride, 10 mM potassium bicarbonate, and 0.1 mM EDTA at pH 7.2). Isolated BM cells were kept in Dulbecco's PBS or complete RPMI-1640 medium (RPMI-1640 medium containing 10% fetal calf serum, 2 mM L-glutamine, 100 U/ml penicillin, and 100 μg/ml streptomycin) until further use.

Assessment of $(Ca^{2+})_i$ changes in BM neutrophils

In this assay, the increase in $(Ca^{2+})_i$ concentration of neutrophils ($Ly6G^+$ cells) from isolated BM cells from *C57BL/6J* (WT), *C5ar1*$^{-/-}$, and *C5ar2*$^{-/-}$ (both on *C57BL/6J* background) mice was measured after stimulation with recombinant C5a (Hycult Biotech, Uden, Netherlands), as previously described (Karsten et al., 2014). Briefly, after staining of the cells with neutrophil surface markers and the calcium-sensitive compound Fluo-4, changes in $(Ca^{2+})_i$ concentration were detected by measuring the change in the FITC signal from $Ly6G^+$ cells on a BD LSRII flow cytometer (BD Biosciences, Franklin Lakes, NJ) after the addition of C5a to a final concentration of 0.2 nM. The increase in $(Ca^{2+})_i$ concentration was quantified by calculating the relative increase in the AUC of the Fluo-4 signal after the addition of C5a. Details are mentioned in Supplementary Materials and Methods.

ROS release assay

In this assay, intra- and extracellular ROS of neutrophils was measured using luminol-amplified chemiluminescence after stimulation with ICs or various controls, on the basis of previous descriptions (Yu et al., 2010). Briefly, white 96-microwell plates (Greiner Bio-One, Frickenhausen, Germany) were coated with mCOL7C/α-mCOL7 IgG ICs. After washing with blocking buffer, 200 μl of freshly isolated BM cells (2.5×10^6 cells/ml in CL medium) were added per well. Finally, luminol (Sigma-Aldrich, St. Louis, MO) was added to each well at a final concentration of 100 μg/ml. mCOL7C or α-mCOL7 alone was used as negative controls. Phorbol-12-myristate-13-acetate (Sigma-Aldrich) at a final concentration of 10 μg/ml was used as a positive control. Luminescence, corresponding to the amount of ROS released, was measured using a Fluostar Omega ELISA reader (BMG LABTECH, Ortenberg, Germany). ROS release was quantified as the increase in the AUC of luminescence relative to the positive control AUC (phorbol-12-myristate-13-acetate). Details are mentioned in Supplementary Materials and Methods.

Neutrophil chemotaxis assay

The chemotactic behavior of neutrophils ($Ly6G^+$ cells) from *C57BL/6J* (WT), *C5ar1*$^{-/-}$, and *C5ar2*$^{-/-}$ (both on *C57BL/6J* background) mice toward C5a was assayed using transwell inserts, as previously described (Xia et al., 2019). Briefly, 2×10^6 isolated BM cells were seeded onto a transwell insert with 3 μm pores (Corning, Kennebunk, ME). C5a was added to the bottom well at a final concentration of 12.5 nM, and cells were incubated at 37 °C, 5% carbon dioxide for 3 hours. Nonmigrated cells from the transwell insert and migrated cells from the bottom well were recovered, stained for Ly6G, and analyzed using a BD LSRII flow cytometer. The percentage of chemotactic neutrophils was calculated by dividing the number of migrated $Ly6G^+$ cells by the total number of recovered neutrophils from the transwell insert and the respective bottom well. As a control, isolated BM cells were seeded onto a transwell insert without the addition of C5a to the bottom well to correct for cells that passed through the pores due to chemokinesis.

Statistical analysis

Statistical analysis of data was performed using GraphPad Prism version 9.2.0 (GraphPad Software, San Diego, CA). All data in the graphs are presented as means ± SEM. *P*-values were determined by unpaired *t*-tests for comparisons between two independent groups, ordinary one-way ANOVA with Holm-Šídák multiple comparison test for comparisons between more than two independent groups, and two-way ANOVA with Holm-Šídák multiple comparison test for comparisons including different time points or expression levels of different markers. Differences between groups were considered significant if the *P*-value was <0.05 (*$P < 0.05$, **$P < 0.01$, ***$P < 0.001$, and ****$P < 0.0001$).

Data availability statement

No datasets were generated or analyzed during this study.

ORCIDs

Daniel Leonard Seiler: http://orcid.org/0000-0001-5533-9237
Marie Kleingarn: http://orcid.org/0000-0002-2291-4693
Katja Hendrika Kähler: http://orcid.org/0000-0001-7356-3494
Caroline Gruner: http://orcid.org/0000-0003-4596-4455
Jovan Schanzenbacher: http://orcid.org/0000-0001-5956-1142
Elvira Ehlers-Jeske: http://orcid.org/0000-0002-8223-0779
Samyr Kenno: http://orcid.org/0000-0002-9448-7344
Christian David Sadik: http://orcid.org/0000-0001-6701-048X
Enno Schmidt: http://orcid.org/0000-0002-1206-8913
Katja Bieber: http://orcid.org/0000-0002-3855-6683
Jörg Köhl: http://orcid.org/0000-0003-1121-3178
Ralf J. Ludwig: http://orcid.org/0000-0002-1394-1737
Christian Marcel Karsten: http://orcid.org/0000-0003-3893-5277

CONFLICT OF INTEREST

The authors state no conflict of interest.

ACKNOWLEDGMENTS

DLS wishes to thank Claudia Kemper and Andreas Hutloff for critical feedback on the revised manuscript and all colleagues who contributed to this study. The study was supported by CRU303 TP4 given to CMK and ES. The grant number is KA 2812/2-1.

AUTHOR CONTRIBUTIONS

Conceptualization: CMK, DLS, RJL, CDS, JK, ES; Funding Acquisition: CMK, ES; Investigation: DLS, MK, KHK, CG, JS, EEJ; Project Administration: DLS, CMK; Resources: RJL, KB, JK, SK; Supervision: DLS, CMK; Writing - Original Draft Preparation: DLS; Writing - Review and Editing: DLS, RJL, ES, SK, JK, CDS, CMK

SUPPLEMENTARY MATERIAL

Supplementary material is linked to the online version of the paper at www.jidonline.org, and at https://doi.org/10.1016/j.jid.2021.12.029.

REFERENCES

Atkinson JP. C5a and Fcγ receptors: a mutual admiration society. J Clin Invest 2006;116:304–6.

Bamberg CE, Mackay CR, Lee H, Zahra D, Jackson J, Lim YS, et al. The C5a receptor (C5aR) C5L2 is a modulator of C5aR-mediated signal transduction. J Biol Chem 2010;285:7633–44.

Bieber K, Ludwig RJ. Drug development in pemphigoid diseases. Acta Derm Venereol 2020;100:adv00055.

Bussel JB. Fc receptor blockade and immune thrombocytopenic purpura. Semin Hematol 2000;37:261–6.

Chen NJ, Mirtsos C, Suh D, Lu YC, Lin WJ, McKerlie C, et al. C5L2 is critical for the biological activities of the anaphylatoxins C5a and C3a. Nature 2007;446:203–7.

Chiriac MT, Roesler J, Sindrilaru A, Scharffetter-Kochanek K, Zillikens D, Sitaru C. NADPH oxidase is required for neutrophil-dependent autoantibody-induced tissue damage. J Pathol 2007;212:56–65.

Chou RC, Kim ND, Sadik CD, Seung E, Lan Y, Byrne MH, et al. Lipid-cytokine-chemokine cascade drives neutrophil recruitment in a murine model of inflammatory arthritis. Immunity 2010;33:266–78.

Croker DE, Halai R, Fairlie DP, Cooper MA. C5a, but not C5a-des Arg, induces upregulation of heteromer formation between complement C5a receptors C5aR and C5L2. Immunol Cell Biol 2013;91:625–33.

Croker DE, Halai R, Kaeslin G, Wende E, Fehlhaber B, Klos A, et al. C5a2 can modulate ERK1/2 signaling in macrophages via heteromer formation with C5a1 and β-arrestin recruitment. Immunol Cell Biol 2014;92:631–9.

Croker DE, Monk PN, Halai R, Kaeslin G, Schofield Z, Wu MC, et al. Discovery of functionally selective C5aR2 ligands: novel modulators of C5a signalling. Immunol Cell Biol 2016;94:787–95.

Gerard NP, Lu B, Liu P, Craig S, Fujiwara Y, Okinaga S, et al. An anti-inflammatory function for the complement anaphylatoxin C5a-binding protein, C5L2. J Biol Chem 2005;280:39677–80.

Girardi G, Berman J, Redecha P, Spruce L, Thurman JM, Kraus D, et al. Complement C5a receptors and neutrophils mediate fetal injury in the antiphospholipid syndrome [published correction appears in J Clin Invest 2003;113:646]. J Clin Invest 2003;112:1644–54.

Godau J, Heller T, Hawlisch H, Trappe M, Howells E, Best J, et al. C5a initiates the inflammatory cascade in immune complex peritonitis. J Immunol 2004;173:3437–45.

Kalant D, MacLaren R, Cui W, Samanta R, Monk PN, Laporte SA, et al. C5L2 is a functional receptor for acylation-stimulating protein. J Biol Chem 2005;280:23936–44.

Karsten CM, Beckmann T, Holtsche MM, Tillmann J, Tofern S, Schulze FS, et al. Tissue destruction in bullous pemphigoid can be complement independent and may be mitigated by C5aR2. Front Immunol 2018;9:488.

Karsten CM, Köhl J. The immunoglobulin, IgG Fc receptor and complement triangle in autoimmune diseases. Immunobiology 2012;217:1067–79.

Karsten CM, Laumonnier Y, Köhl J. Functional analysis of C5a effector responses in vitro and in vivo. Methods Mol Biol 2014;1100:291–304.

Karsten CM, Pandey MK, Figge J, Kilchenstein R, Taylor PR, Rosas M, et al. Anti-inflammatory activity of IgG1 mediated by Fc galactosylation and association of FcγRIIB and dectin-1. Nat Med 2012;18:1401–6.

Karsten CM, Wiese AV, Mey F, Figge J, Woodruff TM, Reuter T, et al. Monitoring C5aR2 expression using a floxed tdTomato-C5aR2 knock-in mouse. J Immunol 2017;199:3234–48.

Kasperkiewicz M, Nimmerjahn F, Wende S, Hirose M, Iwata H, Jonkman MF, et al. Genetic identification and functional validation of FcγRIV as key molecule in autoantibody-induced tissue injury. J Pathol 2012;228:8–19.

Kasperkiewicz M, Sadik CD, Bieber K, Ibrahim SM, Manz RA, Schmidt E, et al. Epidermolysis bullosa acquisita: from pathophysiology to novel therapeutic options. J Invest Dermatol 2016;136:24–33.

Kasprick A, Bieber K, Ludwig RJ. Drug discovery for pemphigoid diseases. Curr Protoc Pharmacol 2019;84:e55.

Koga H, Prost-Squarcioni C, Iwata H, Jonkman MF, Ludwig RJ, Bieber K. Epidermolysis bullosa acquisita: the 2019 update. Front Med 2019;5:362.

Kovacs B, Tillmann J, Freund LC, Nimmerjahn F, Sadik CD, Bieber K, et al. Fcγ receptor IIB controls skin inflammation in an active model of epidermolysis bullosa acquisita. Front Immunol 2020;10:3012.

Kumar V, Ali SR, Konrad S, Zwirner J, Verbeek JS, Schmidt RE, et al. Cell-derived anaphylatoxins as key mediators of antibody-dependent type II autoimmunity in mice. J Clin Invest 2006;116:512–20.

Lajoie S, Lewkowich IP, Suzuki Y, Clark JR, Sproles AA, Dienger K, et al. Complement-mediated regulation of the IL-17A axis is a central genetic determinant of the severity of experimental allergic asthma. Nat Immunol 2010;11:928–35.

Looney MR, Su X, Van Ziffle JA, Lowell CA, Matthay MA. Neutrophils and their Fc gamma receptors are essential in a mouse model of transfusion-related acute lung injury. J Clin Invest 2006;116:1615–23.

Mihai S, Hirose M, Wang Y, Thurman JM, Holers VM, Morgan BP, et al. Specific inhibition of complement activation significantly ameliorates autoimmune blistering disease in mice. Front Immunol 2018;9:535.

Miyabe Y, Miyabe C, Mani V, Mempel TR, Luster AD. Atypical complement receptor C5aR2 transports C5a to initiate neutrophil adhesion and inflammation. Sci Immunol 2019;4:eaav5951.

Nimmerjahn F, Ravetch JV. Fcgamma receptors: old friends and new family members. Immunity 2006;24:19–28.

Nimmerjahn F, Ravetch JV. Fcgamma receptors as regulators of immune responses. Nat Rev Immunol 2008;8:34–47.

Nishie W. Update on the pathogenesis of bullous pemphigoid: an autoantibody-mediated blistering disease targeting collagen XVII. J Dermatol Sci 2014;73:179–86.

Ohno M, Hirata T, Enomoto M, Araki T, Ishimaru H, Takahashi TA. A putative chemoattractant receptor, C5L2, is expressed in granulocyte and immature dendritic cells, but not in mature dendritic cells. Mol Immunol 2000;37:407–12.

Okinaga S, Slattery D, Humbles A, Zsengeller Z, Morteau O, Kinrade MB, et al. C5L2, a nonsignaling C5A binding protein. Biochemistry 2003;42:9406–15.

Poppelaars F, van Werkhoven MB, Kotimaa J, Veldhuis ZJ, Ausema A, Broeren SGM, et al. Critical role for complement receptor C5aR2 in the pathogenesis of renal ischemia-reperfusion injury. FASEB J 2017;31:3193–204.

Ricklin D, Hajishengallis G, Yang K, Lambris JD. Complement: a key system for immune surveillance and homeostasis. Nat Immunol 2010;11:785–97.

Rittirsch D, Flierl MA, Nadeau BA, Day DE, Huber-Lang M, Mackay CR, et al. Functional roles for C5a receptors in sepsis. Nat Med 2008;14:551–7.

Sadik CD, Kim ND, Iwakura Y, Luster AD. Neutrophils orchestrate their own recruitment in murine arthritis through C5aR and FcγR signaling. Proc Natl Acad Sci USA 2012;109:E3177–85.

Sadik CD, Miyabe Y, Sezin T, Luster AD. The critical role of C5a as an initiator of neutrophil-mediated autoimmune inflammation of the joint and skin. Semin Immunol 2018;37:21–9.

Sadik CD, Schmidt E, Zillikens D, Hashimoto T. Recent progresses and perspectives in autoimmune bullous diseases. J Allergy Clin Immunol 2020;145:1145–7.

Samavedam UKSRL, Iwata H, Müller S, Schulze FS, Recke A, Schmidt E, et al. GM-CSF modulates autoantibody production and skin blistering in experimental epidermolysis bullosa acquisita. J Immunol 2014;192:559–71.

Schmidt E, Zillikens D. Pemphigoid diseases. Lancet 2013;381:320–32.

Schmidt RE, Gessner JE. Fc receptors and their interaction with complement in autoimmunity. Immunol Lett 2005;100:56–67.

Schulze FS, Beckmann T, Nimmerjahn F, Ishiko A, Collin M, Köhl J, et al. Fcγ receptors III and IV mediate tissue destruction in a novel adult mouse model of bullous pemphigoid. Am J Pathol 2014;184:2185–96.

Sezin T, Krajewski M, Wutkowski A, Mousavi S, Chakievska L, Bieber K, et al. The leukotriene B_4 and its receptor BLT1 act as critical drivers of neutrophil recruitment in murine bullous pemphigoid-like epidermolysis bullosa acquisita. J Invest Dermatol 2017;137:1104–13.

Sezin T, Murthy S, Attah C, Seutter M, Holtsche MM, Hammers CM, et al. Dual inhibition of complement factor 5 and leukotriene B_4 synergistically suppresses murine pemphigoid disease. JCI Insight 2019;4:e128239.

Shimanovich I, Mihai S, Oostingh GJ, Ilenchuk TT, Bröcker EB, Opdenakker G, et al. Granulocyte-derived elastase and gelatinase B are required for dermal-epidermal separation induced by autoantibodies from patients with epidermolysis bullosa acquisita and bullous pemphigoid. J Pathol 2004;204:519–27.

Shushakova N, Skokowa J, Schulman J, Baumann U, Zwirner J, Schmidt RE, et al. C5a anaphylatoxin is a major regulator of activating versus inhibitory FcgammaRs in immune complex-induced lung disease. J Clin Invest 2002;110:1823–30.

Sitaru C, Mihai S, Otto C, Chiriac MT, Hausser I, Dotterweich B, et al. Induction of dermal-epidermal separation in mice by passive transfer of antibodies specific to type VII collagen. J Clin Invest 2005;115:870–8.

Thorenz A, Derlin K, Schröder C, Dressler L, Vijayan V, Pradhan P, et al. Enhanced activation of interleukin-10, heme oxygenase-1, and AKT in C5aR2-deficient mice is associated with protection from ischemia reperfusion injury–induced inflammation and fibrosis. Kidney Int 2018;94:741–55.

Tonnesen MG, Smedly LA, Henson PM. Neutrophil-endothelial cell interactions. Modulation of neutrophil adhesiveness induced by complement fragments C5a and C5a des arg and formyl-methionyl-leucyl-phenylalanine in vitro. J Clin Invest 1984;74:1581–92.

Van Lith LH, Oosterom J, Van Elsas A, Zaman GJ. C5a-Stimulated recruitment of beta-arrestin2 to the nonsignaling 7-transmembrane decoy receptor C5L2. J Biomol Screen 2009;14:1067–75.

Wang R, Lu B, Gerard C, Gerard NP. Disruption of the complement anaphylatoxin receptor C5L2 exacerbates inflammation in allergic contact dermatitis. J Immunol 2013;191:4001–9.

Wipke BT, Allen PM. Essential role of neutrophils in the initiation and progression of a murine model of rheumatoid arthritis. J Immunol 2001;167:1601–8.

Wu MCL, Lee JD, Ruitenberg MJ, Woodruff TM. Absence of the C5a receptor C5aR2 worsens ischemic tissue injury by increasing C5aR1-mediated neutrophil infiltration. J Immunol 2020;205:2834–9.

Xia BT, Beckmann N, Winer LK, Pugh AM, Pritts TA, Nomellini V, et al. Amitriptyline reduces inflammation and mortality in a murine model of sepsis. Cell Physiol Biochem 2019;52:565–79.

Yu X, Holdorf K, Kasper B, Zillikens D, Ludwig RJ, Petersen F. FcγRIIA and FcγRIIIB are required for autoantibody-induced tissue damage in experimental human models of bullous pemphigoid [published correction appears in J Invest Dermatol 2012;132:1938]. J Invest Dermatol 2010;130:2841–4.

Zhang T, Garstka MA, Li K. The controversial C5a receptor C5aR2: its role in health and disease [published correction appears in J Immunol Res 2017;2017:6073961]. J Immunol Res 2017;2017:8193932.

Zhang X, Schmudde I, Laumonnier Y, Pandey MK, Clark JR, König P, et al. A critical role for C5L2 in the pathogenesis of experimental allergic asthma. J Immunol 2010;185:6741–52.

SUPPLEMENTARY MATERIALS AND METHODS

Antibodies

For the antibody transfer model, rabbit anti-murine type VII collagen IgG was used, which was produced and purified as described (Bieber et al., 2016). For direct immunofluorescence, FITC-conjugated anti-rabbit IgG (8.33 μg/ml; Dako Deutschland, Hamburg, Germany) and FITC-labeled anti-mouse C3 (66.6 μg/ml; Cappel, MP Biomedicals, Solon, OH) were used. DAPI (5 mg/ml; Life Technologies, Carlsbad, CA) was used to stain the nuclei in all immunofluorescence staining. For flow cytometric analyses, FcγRs were blocked with anti-mouse CD16/CD32 (5 μg/ml; 93, Life Technologies). In addition, PE-Cy7-conjugated anti-mouse Ly6G (1 μg/ml; RB6-8C5, eBioscience, San Diego, CA), PerCP-Cy5.5-labeled anti-mouse CD45 (2 μg/ml; 30-F11, eBioscience), APC-conjugated anti-mouse Ly6G (1 μg/ml; 1A8, BioLegend, San Diego, CA), V450-labeled anti-mouse Ly6G (1 μg/ml; 1A8, BD), AF700-conjugated anti-mouse CD11b (2 μg/ml; M1/70, eBioscience), BV510-labeled anti-mouse CD11b (1 μg/ml; M1/70, BioLegend), PE-conjugated anti-mouse FcγRI (1 μg/ml; X54-5/7.1, BioLegend), FITC-labeled anti-mouse FcγRIIb (8.33 μg/ml; Ly17.2, kindly provided by Falk Nimmerjahn), and APC-conjugated anti-mouse FcγRIV (1 μg/ml; 9E9, BioLegend) were used. In addition, APC-labeled rat IgG2a, κ isotype control (1 μg/ml; RTK2758, BioLegend) and AF700- and PerCP-Cy5.5-conjugated rat IgG2b, κ isotype controls (2 μg/ml; eB149/10H5, eBioscience) were used to identify nonspecific binding. Dead cells were stained with the amine-reactive fixable viability dye eFluor 780 (Life Technologies).

Assessment of intracellular calcium changes in bone marrow neutrophils

For staining of cells with the calcium-sensitive compound Fluo-4, isolated bone marrow cells were resuspended to a final concentration of 1×10^7 cells/ml in Dulbecco's PBS and incubated with 10 μM Fluo-4 AM in the dark for 30 minutes at room temperature. After a wash step with 500 μl Dulbecco's PBS, the incubation step was repeated to allow intracellular esterases to hydrolyze the acetoxymethyl, unmasking the negatively charged carboxylate groups on the fluorescent compound, making it cell-impermeant and therefore well-retained in the cytoplasm. For detecting changes in intracellular calcium concentration in $Ly6G^+$ cells on a BD LSRII flow cytometer (BD Biosciences, Franklin Lakes, NJ), baseline fluorescence was acquired for 15 seconds before the sample tube was removed from the flow cytometer without stopping the measurement and then C5a was added (0.2 nM final concentration), and the tube was quickly reconnected to the flow cytometer. The fluorescence signal was monitored for 2.5 minutes, then 0.5 μg of ionomycin was added as a positive control, and the measurement was continued for another 2.25 minutes. The Fluo-4 signal in $Ly6G^+$-gated bone marrow cells, in response to C5a and ionomycin, was transformed into a time-dependent curve using the Kinetics tool within the FlowJo software (version 10; Tree Star, Ashland, OR).

Neutrophil CD11b upregulation assay

To investigate the activation potential of neutrophils ($Ly6G^+$ cells) from *C57BL/6J* (wild-type) and *C5ar2*$^{-/-}$ (in *C57BL/6J* background) mice after stimulation with C5a, changes in the surface expression of the activation marker CD11b were quantified by flow cytometry. In brief, isolated bone marrow cells were incubated in a complete RPMI-1640 medium containing 2.5 nM C5a or no C5a as a control for 30 minutes at 37 °C, 5% carbon dioxide. Cells were washed and stained for Ly6G and CD11b after blocking FcγRs with anti-FcγRII (CD32) and anti-FcγRIII (CD16) antibodies. CD11b expression of C5a-stimulated and nonstimulated $Ly6G^+$ cells were determined using a BD LSRII flow cytometer. Changes in CD11b expression were quantified by calculating the relative increase in mean fluorescence intensity of the CD11b signal in response to C5a stimulation.

ROS release assay

White 96-microwell plates (Greiner Bio-One, Frickenhausen, Germany) were coated with 1 μg recombinant murine type VII collagen C per well at 4 °C overnight. After blocking with blocking buffer (Dulbecco's PBS, 1% BSA, 0.05% [w/v] Tween-20) at room temperature for at least 1 hour, 0.2 μg affinity-purified rabbit anti-murine type VII collagen IgG per well was incubated with the plates at room temperature for 1.5 hours. After washing with blocking buffer, 100 μl CL medium (RPMI-1640 medium without phenol red and 10% fetal calf serum and with L-glutamine and 25 mM 4-[2-hydroxyethyl]-1-piperazineethanesulfonic acid) was added to each well, followed by 100 μl of freshly isolated bone marrow cells (5×10^6 cells/ml in CL medium). After the addition of luminol (Sigma-Aldrich, St. Louis, MO), luminescence, corresponding to the amount of ROS released in the form of hydroxide ion, oxygen ion, and hydrogen peroxide, was measured every 2 minutes for 2 hours using a Fluostar Omega ELISA reader (BMG LABTECH, Ortenberg, Germany) at an absorbance rate of up to 3,600 and an average measurement interval of 1 second at 37 °C.

Isolation and flow cytometric analysis of immune cells from murine ears

To quantify the number of neutrophils infiltrating the skin, right ears were harvested from diseased *C57BL/6J* (wild-type) and *C5ar2*$^{-/-}$ (on *C57BL/6J* background) mice, and immune cells were isolated by mechanical and enzymatic digestion. In brief, the dorsal part of the ear was cut into small fragments and then incubated in complete RPMI-1640 medium containing 1 mg/ml collagenase IV and 50 U/ml DNase I at 37 °C, 300 r.p.m. for 50 minutes. Enzymatic digestion was stopped by adding 0.25 M EDTA in a complete RPMI-1640 medium. The cell suspension and remaining tissue were then mashed through a 40-μm cell strainer into a 50-ml tube using the plunger of a 5-ml syringe. Isolated cells were centrifuged and stained for CD45, Ly6G, and CD11b. Surface expression of these antigens was analyzed using a Cytek Aurora spectral analyzer (Cytek Biosciences, Fremont, CA). Autofluorescence was subtracted, and isotype and fluorescence minus one controls were used to identify specific antibody binding.

SUPPLEMENTARY REFERENCE

Bieber K, Witte M, Sun S, Hundt JE, Kalies K, Dräger S, et al. T cells mediate autoantibody-induced cutaneous inflammation and blistering in epidermolysis bullosa acquisita. Sci Rep 2016;6:38357.

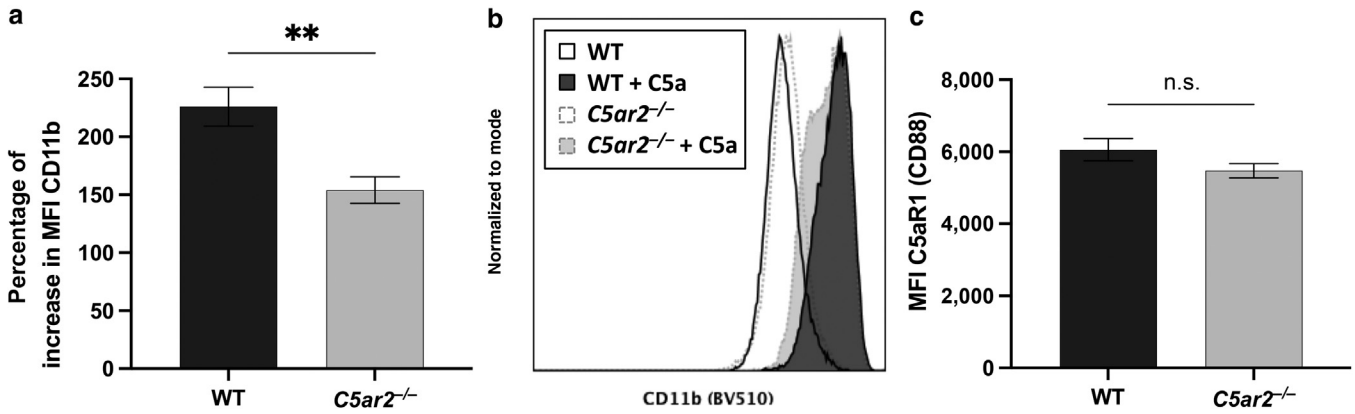

Supplementary Figure S1. C5aR1 (CD88) expression and C5a-induced upregulation of CD11b on BM-derived neutrophils from diseased mice. (**a**) C5a-mediated activation of neutrophils from diseased mice quantified by upregulation of surface expression of CD11b (n = 10 per group). (**b**) Representative histograms showing the C5a-induced upregulation of CD11b. (**c**) Quantitative assessment of C5aR1 (CD88) surface expression in Ly6G$^+$ BM cells from diseased mice (n = 10 per group). Shown are combined data from two independent experiments, each performed with five mice per genotype. Differences between groups were analyzed by unpaired two-tailed *t*-test. BM, bone marrow; MFI, mean fluorescence intensity; n.s., not significant; WT, wild-type. $^{**}P < 0.01$.

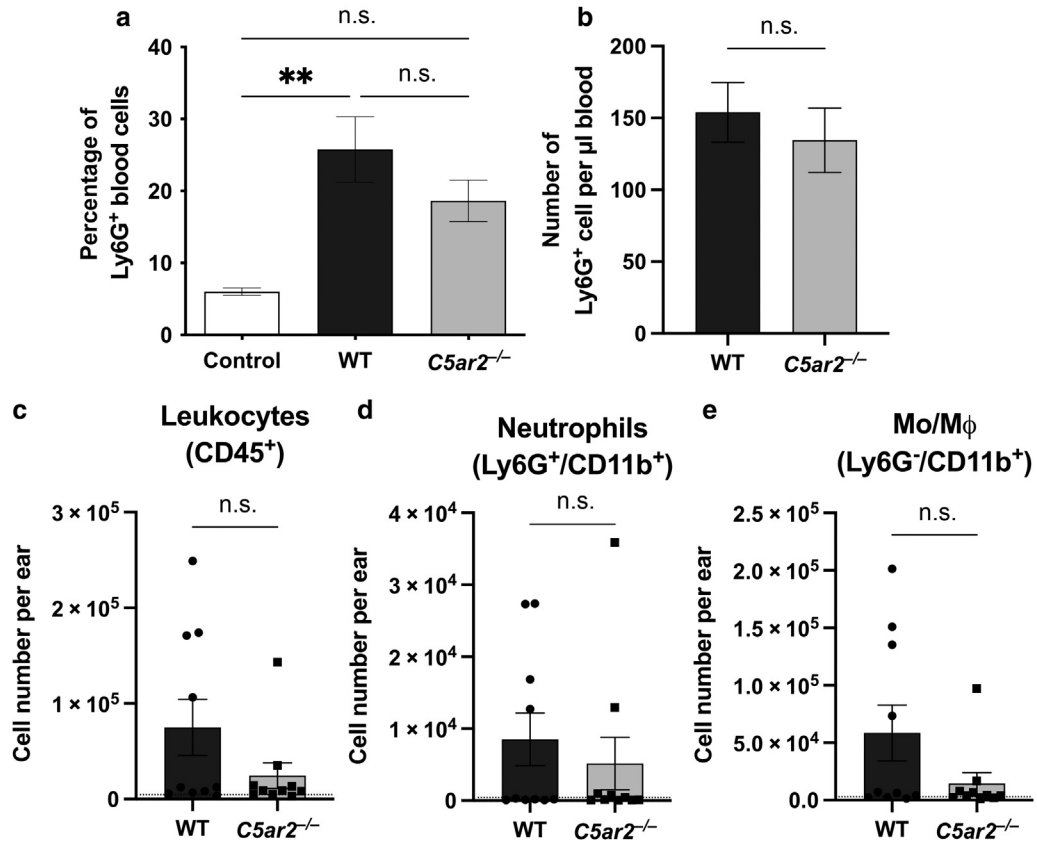

Supplementary Figure S2. The number of neutrophils in the blood and infiltrating immune cells in the ears is elevated in diseased mice of both genotypes (WT and *C5ar2*$^{-/-}$). (**a, b**) *C5ar2*$^{-/-}$ mice show a tendency to a decreased number of neutrophils in the blood compared with WT mice, although the differences are not significant (**a**: $P = 0.0522$; n = 11 for WT and *C5ar2*$^{-/-}$, n = 7 for control; **b**: n = 10 per group). (**c**–**e**) The number of infiltrating immune cells tended to be lower in diseased *C5ar2*$^{-/-}$ mice, but significance was not reached (n = 10 per group; the dotted line in each graph represents the number of immune cells in the ears of naive, nondiseased mice, which is similar in WT and *C5ar2*$^{-/-}$ mice). Differences between groups were analyzed by ordinary one-way ANOVA with Holm-Šídák multiple comparisons test for (**a**), and by unpaired one-tailed *t*-test for (**b**–**e**). n.s., not significant; WT, wild-type. $^{**}P < 0.01$.